Impact of "chemical cocktails" exposure in shaping mice gut microbiota and the role of selenium supplementation combining metallomics, metabolomics, and metataxonomics

A. Arias-Borrego [a,b], M. Selma-Royo [c], M.C. Collado [c,1], N. Abril [d,1], T. García-Barrera [a,*,1]

[a] Research Center of Natural Resources, Health and the Environment (RENSMA). Department of Chemistry, Faculty of Experimental Sciences, University of Huelva, Fuerzas Armadas Ave., 21007 Huelva, Spain
[b] Department of Analytical Chemistry, Faculty of Chemistry, University of Sevilla, 41012 Sevilla, Spain
[c] Institute of Agrochemistry and Food Technology (IATA-CSIC), Department of Biotechnology, Agustin Escardino 7, 46980 Paterna, Valencia, Spain
[d] Department of Biochemistry and Molecular Biology, University of Córdoba, Campus de Rabanales, Edificio Severo Ochoa, E-14071 Córdoba, Spain

HIGHLIGHTS

- "Chemical cocktail" exposure affected plasma selenoproteome and gut microbiota.
- "Chemical cocktail" exposure affected plasma metabolome and arsenic metabolization.
- Selenium partially antagonize the exposure to antibiotics and "chemical cocktails".
- The potential beneficial role of selenium could be intertwined with gut microbiota.
- Crucial role of microbiota in the physiological response to "chemical cocktails" is suggested.

GRAPHICAL ABSTRACT
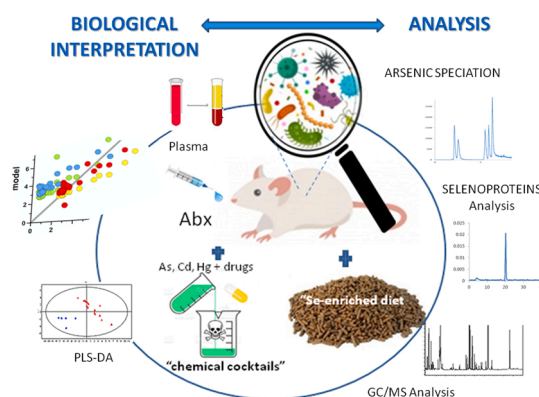
ARTICLE INFO

Editor: Jörg Rinklebe

Keywords:
Selenium
Selenoproteins

ABSTRACT

Biological systems are exposed to a complex environment in which pollutants can interact through synergistic or antagonistic mechanisms, but limited information is available on the combined effects. To this end, conventional and antibiotic-treated (Abx) mice models were fed regular rodent or selenium (Se) supplemented diets and exposed to a "chemical cocktail" (CC) including metals and pharmaceuticals. Metallomics, metabolomics, and metataxomics were combined to delve into the impact on gut microbiota, plasma selenoproteome, metabolome,

and arsenic metabolization. At the molecular level, Se decreased the concentration of the antioxidant glutathione peroxidase in plasma and increased the arsenic methylation rate, possibly favoring its excretion, but not in the Abx and also plasma metabolomes of Abx, and Abx-Se were not differentiated. Moreover, numerous associations were obtained between plasma selenoproteins and gut microbes. Se-supplementation partially antagonizes the gut microbiota alteration caused by Abx, and slightly by CC, but strongly altered profiles were observed in CC-Abx-Se, suggesting synergistic deleterious effects between pollutants, Abx and Se. Moreover, although CC and Abx changed gut microbiota, several common taxa were enriched in CC-Abx and control mice, indicating possible synergistic effects. Our results suggest a potential beneficial impact of supplementation, but mediated by gut microbes being reversed in their absence.

1. Introduction

Free-living environmental bioindicators or laboratory animal models are frequently used to assess the physiological response to biomarkers of environmental pollution (García-Barrera et al., 2012). Mammals are usually preferred to be compared with humans since the digestive tract is also present, which is an important biological filter for the absorption of pollutants that finally reach the bloodstream and are distributed to the organs (García-Barrera et al., 2018). Exposure experiments to "chemical cocktails" (CC) that incorporate environmental pollutants from different compound classes allow evaluating the real effects of contaminants in the environment (Van Genderen et al., 2015) since they usually interact through antagonistic or synergistic mechanisms (García-Barrera et al., 2012). Selenium (Se) is a non-metal with certain metalloid properties very important for health (e.g., cancer, diabetes) (Rayman, 2012) and a well-known antagonist against many pollutants in mammals. Likewise, Se antagonizes cardiovascular damages (Park and Mozaffarian, 2010), neurotoxicity (Choi et al., 2008), and renal toxicity (Beyrouty and Chan, 2006) induced by mercury (Hg) as well as skin cancer (Kolachi et al., 2011) and DNA hypomethylation (George et al., 2013) caused by arsenic (As). Synergistic interactions have been described between cadmium (Cd) and As producing more marked renal toxicity in humans than the isolated exposure to each of them (Nordberg et al., 2005) and inducing lipid peroxidation, glutathione and metallothionein, and redistribution of essential elements in rats (Yáñez et al., 1991). Otherwise, Se prevents oxidative stress (Messaoudi et al., 2009), nephrotoxicity, hepatotoxicity (Flora et al., 1982), and chromosomal aberrations (Mukherjee et al., 1988) induced by Cd. Se also presents protective roles against the deleterious effects induced by organic pollutants, such as the lipid peroxidation and oxidative stress triggered by organophosphorus pesticides (Milošević et al., 2017), the metabolic damages triggered by the pesticide p,p′-dichloro diphenyl trichloroethane (DDE) (Rodríguez-Moro et al., 2019) and diclofenac (DCF)-induced decreases in testicular function enzymes, sperm motility and count and the concentration of serum testosterone and luteinizing hormone (Owumi et al., 2020). Numerous metallomic and metabolomic studies in mice demonstrated the role of Se against the isolated exposure to Hg (García-Sevillano et al., 2015), As (García-Sevillano et al., 2013, 2014a), and Cd (García-Sevillano et al., 2014b), but little information is available on joint exposure to these contaminants as it is likely to occur in the environment.

The human microbiota is formed by a complex and dynamic bacterial community that plays key roles in health, intervening in important physiological, metabolic, and immunological functions of the host. Recent studies demonstrate the influence of Se-supplementation on mice gut microbiota, plasma selenoproteome, and metal homeostasis (Callejón-Leblic et al., 2021) as well as on gut metabolites (Callejón-Leblic et al., 2022). Moreover, the link between metal oral exposure and mice gut microbiota has been pointed out (Zhai et al., 2017), as well as the potential role of the latter against the absorption of heavy metals (Collado et al., 2015). However, limited information is available on the CC of contaminants to delve into the global influence of those on the microbiota nor the interaction with Se intertwined with the latter.

Herein we describe the evaluation of the impact of a mixture

including As, Cd, Hg, and pharmaceutically active compounds (PACs, flumequine, and DCF) on mice gut microbiota and the role of Se supplementation on its effect. Plasma selenoproteome, As species, and metabolites were analyzed and compared between mice exposed to the pollutants fed a regular rodent diet and Se supplemented diet. Non-targeted metabolomics analysis was accomplished by gas chromatography coupled to mass spectrometry (GC-MS), while speciation of As and selenoproteins was performed by ultra-high performance liquid chromatography (UHPLC) with inductively coupled plasma mass spectrometry (ICP-MS). Gut microbiota profiling was determined by 16S rRNA amplicon sequencing using Illumina technology. We combined the use of conventional mice and microbiota-depleted mice with antibiotics to delve into the potential role of Se-supplementation in mice models after exposure to the pollutant mixture.

2. Experimental section

2.1. Animals, dosage information and experimental design

Mus musculus BALB/c (8 weeks old, n = 60) male mice, obtained from Charles River, were allowed to acclimate to a conventional facility for 3 days with a 12-hour light-dark cycle and *ad libitum* access to both drinking water and regular rodent diet. Mice were then randomly divided into five groups: C, CC, CC-Se, CC-Abx, CC-Abx-Se, and hosed in pairs. During the first next week, all mice were fed a standard murine diet (Se content: 0.2 mg/kg), and mice in groups CC-Abx, CC-Abx-Se also received a mixture of antibiotics in the drinking water. The antibiotic cocktail contained metronidazole 1%, ampicillin 1%, vancomycin 0.5%, neomycin 1%, and an antifungal (amphotericin B, 10 mg/L), enough to change gut microbiota and affect the host metabolism (Callejón-Leblic et al., 2021; Zarrinpar et al., 2018; D'Amato et al., 2020). During the next two following weeks, all mice except those included in the C (control) group received an up to five pollutants in the chow (diclofenac-DCF and flumequine-FLQ) and in the drinking water (As, Cd, and Hg) and the mice in the groups CC-Se and CC-Abx-Se, also received a Se supplement (0.65 mg/kg) (Zarrinpar et al., 2018; D'Amato et al., 2020).

The concentrations of DCF and FLQ in the diet were calculated for mice receiving daily doses of 20 mg/kg and 625 mg/kg, respectively. The concentrations of Cd, As and Hg in the drinking water were calculated for mice ingesting daily doses of 0.1 mg/kg, 3 mg/kg, and 1 mg/kg, respectively. For the selection of metal and drug doses, we relied on the literature and our previous work (García-Sevillano et al., 2013; Callejón-Leblic et al., 2022; Zhai et al., 2017; Collado et al., 2015; Zarrinpar et al., 2018; D'Amato et al., 2020; López-Pacheco et al., 2019; Kashida et al., 2006; Trombini et al., 2021; Rodríguez-Moro et al., 2020). These used doses are consistent with the concentrations of environmental relevance (Fekadu et al., 2019; González-Gaya et al., 2022; Huygens et al., 2022) and also they are a compromise between the concentrations that are likely to provoke an effect and semi-realistic environmental conditions. In all cases, doses of contaminants below their LD50 were used, as their possible synergistic effects could enhance their toxicity. Finally, mice were anesthetized (isofluorane inhalation) and blood was drawn by cardiac puncture into a heparinized tube. The animals were sacrificed by cervical dislocation and immediately dissected to remove

organs. The investigation was performed in accordance with the current European Union rules and the ARRIVE Guideline (https://arriveguidelines.org/arrive-guidelines) and with the consent of the Ethical Committee of the University of Córdoba (Spain) and the regional government (Ref. 02–01–2019–001).

2.2. Mice plasma selenoproteome

Speciation of plasma selenoproteins was carried out by a previously developed method that allows quantifying the absolute concentration of main plasma selenoproteins namely, selenoprotein P (SELENOP), glutathione peroxidase (GPx), and selenoalbumin (SeAlb). The method is based on a two-dimensional chromatographic separation combining affinity and size exclusion chromatography (2D-SEC-AFC) with inductively coupled plasma mass spectrometry (ICP-MS). Thus, selenoproteins are determined using Se as a "tag" in a sensitive atomic detector instead of a molecular one, which is called heteroatom-tagged proteomics (Sanz-Medel, 2016). The use of an ICP-MS allows the absolute quantification of selenometabolites and selenoproteins by species-unspecific isotopic dilution analysis (IDA) at very low detection limits, which overcome instrumental drift corrections, matrix effects, and preconcentration/dilution factors (Rodríguez-González et al., 2005).

Mice plasma was analyzed as described by Callejón-Leblic et al (Callejón-Leblic et al., 2021). (see the Supporting Information).

2.3. Arsenic speciation in mice plasma

An anion-exchange Hamilton PRP-X100 column (250 length x 2.1 mm I.D., 10 μm particle size) was used to separate arsenic species in mice plasma. A volume of 100 μL of plasma or standard solutions was injected into a sample loop. As species were separated by using a gradient with two mobile phases at 40 ºC: (i) 12.5 mM NH_4HCO_3, pH 9.0 (adjusted with NH_4OH), and 1% MeOH (mobile phase A) and (ii) 60 mM NH_4HCO_3, pH 9.0 (adjusted with NH_4OH), and 1% MeOH (mobile phase B). The mobile phase gradient was as follows: initially, NH_4HCO_3 at 2.5 mM was pumped for 3 min, and then increased to 60 mM in 0.5 min, held for 4.5 min, and decreased to 12.5 mM in 0.5 min. Finally, it was held at this lower concentration for 3.5 min for column re-equilibration before the next injection. The flow rate was maintained at 1.2 mL min^{-1} during a total time of 12 min, required for the separation of all the arsenicals. An 8800 Triple Quad ICP-MS (Agilent Technologies, Tokyo, Japan) coupled with an Agilent 1290 Infinity model UHPLC was used as a specific elemental detector. The operational parameters of ICP-MS were controlled by using a daily tuning solution. As optimized operating conditions were accomplished via direct infusion of 100 μg As L^{-1} standard solution (Merck, Singapore) in 2% (v/v) HNO_3. A PEEK tube was used to connect the UHPLC column to the ICP-MS nebulizer.

As stock solutions for chemical species at 1.0 mg mL^{-1} were prepared by dissolving separately the appropriate amounts in MilliQ water. Sodium arsenite ($NaAsO_2$, ^{III}As) and sodium arsenate dibasic heptahydrate ($Na_2HAsO_4.7 H_2O$, ^{V}As) were purchased by Sigma-Aldrich (Steinheim, Germany), Arsenobetaine (AB), dimethylarsinic acid ($C_2H_7AsO_2$, DMA) and monomethylarsinic acid MA ($C_3H_7AsNa_2O_3$) were obtained from Supelco (Bellefonte, USA). Instrumental six-point external calibration curves were used for the quantification of As species (0.5–100 μg As L^{-1}) under operational parameters of AE-ICP-MS. Figures of merit are collected in Table S1. The LOQ values were comparable to those previously reported in the literature for As speciation related to similar sample matrices and chemical species (Benramdane et al., 1999). The extraction was performed following a previously described method (Nguyen et al., 2018) with several modifications. Briefly, an aliquot of 100 μL of plasma sample was accurately weighed, then, 125 μL of 25% (v/v) trichloroacetic acid was added, it was treated with 20 μL of acetonitrile and 20 μL deionized water, and then, vortex-mixed for 120 s. The mixture was then centrifuged at 10,000 *g* for 10 min at 4 °C and

filtered using a 0.45 μm membrane. The supernatants were injected into the AE-ICP-MS system.

2.4. Untargeted metabolomic analysis

A gas chromatograph model Trace GC ULTRA coupled to a mass spectrometer model ITQ900 (Thermo Fisher Scientific) was used for metabolomics analysis. The chromatographic separation was carried out into a VF-5 MS Factor Four-column (length 30 m × ID 0.25 mm, film thickness 0.25 μm, Agilent Technologies). For the chromatographic separation of metabolites, the oven temperature was initially set at 100ºC for 0.5 min, and then ramped to 320 ºC at 15 ºC/min. In the end, this last temperature was held for 7 min (total time of analysis 22.17 min). A constant helium flow rate of 1 mL min^{-1} was used in the column and the injector oven temperature was fixed at 280 ºC. The ionization in the mass spectrometer was carried out by electronic impact (EI) using 70 eV and full scan mode in the 35–650 *m/z* range. The temperature of the anion source was set at 200ºC. For analysis, 1 μl of the extract was injected in splitless mode. Plasma sample preparation for untargeted metabolomic analysis was based on a single-phase procedure described by Villaseñor et al., 2014 (Villaseñor et al., 2014), with minor modifications (see the Supporting Information) and using a Speedvac concentrator (Thermo Fisher, Waltham, USA). GC-MS raw data were processed with the free access R platform (XCMS software) as described by Arias-Borrego et al (Arias-Borrego et al., 2022). The 11.5 version SIMCA-P software and the 5.0 version MetaboAnalyst (https://www.metaboanalyst.ca/) were used for partial least-squares discriminant analysis (PLS-DA). The values of predictive power (Q^2) and class separation (R^2) were used to confirm the quality of the model. Moreover, data were filtered by a coefficient of signal variation (CV) in quality controls (QCs), considering values lower than 30% as acceptable. Version 08 NIST Mass Spectral Library (>80% probability) and Kovats retention indices (KRIs) were used for the annotation of metabolites. Finally, to identify the most altered pathways between the sample groups metabolic pathways were analyzed by MetaboAnalyst 5.0 online data system.

2.5. Gut microbiota profiling by 16S rRNA amplicon sequencing

Total DNA (100 mg) was obtained from gut contents using the Master-Pure DNA Extraction Kit following the manufacturer's instruction (Epicentre, Madison, WI, US) with some modifications as previously described (Callejón-Leblic et al., 2021). DNA was purified by the DNA Purification Kit (Macherey-Nagel, Duren, Germany) according to the manufacturer's protocol and the concentration was assessed by Qubit® 2.0 Fluorometer (Life Technology, Carlsbad, CA, US).

Microbiota profiling was performed following Illumina protocols by the V3-V4 variable region of the 16S rRNA gene sequencing. Briefly, the NextEra Index Kit (Illumina, San Diego, CA, United States) was used for a multiplexing step and the Bioanalyzer DNA 1000 chip was used to check the amplicons (Agilent Technologies, Santa Clara, CA, United States). Libraries were sequenced using a 2 × 300 bp paired-end run (MiSeq Reagent kit v3) on a MiSeq-Illumina platform (FISABIO sequencing service, Valencia, Spain). Negative controls were included in the DNA extraction and the amplicon generation steps and they were also sequenced. Raw sequences were processed as described previously (Callejón-Leblic et al., 2021). In brief,rResidual adaptors were removed from the raw sequences by use of Trimmomatic software, DADA2 pipeline was followed including the quality filtering and chimera removal steps in the R environment (Core and Team, 2020). Amplicon Sequence Variance (ASV) were taxonomically assigned using Silva v132 database including species-level classification . Samples with less than 1000 reads were eliminated from the final statistical analysis (n = 2).

2.6. Statistical analysis

The differences between groups of samples were evaluated by one-way ANOVA and Tukey test using STATISTICA 8.0 from StatSoft to the concentrations of selenoproteins, arsenic species, and each metabolite of plasma mice from groups C, CC, CC-Se, CC-Abx, and CC-Abx-Se. For multiple comparison corrections, the Benjamini-Hochberg (FDR correction) method was applied to all *p*-values to maintain the false positive rate at the $\alpha = 0.05$ level. Moreover, Spearman correlations between gut microbiota (phylum and genus level) and selenoproteins were calculated using the 4.0.2 version R Software Package Hmisc (Andy, 2008) and correlation matrix plots were obtained.

The microbiota analysis was performed in the R environment using different packages : phyloseq (McMurdie and Holmes, 2013) and vegan (Jari Oksanen et al., 2020) packages as well as the microbiomeanalyst online platform (Chong et al., 2020). Other packages were used for plotting including ggplot2 (Wickham, 2009; Leo Lahti, 2017) ggordiplots (Quensen, 2020), PMCMRplus (Thorsten Pohlert, 2021), microbiome (Leo Lahti, 2017). Alpha-diversity metrics including Chao1 and Shannon indexes were obtained at the ASV level after rarefaction to the minimum reads number (51295 reads, one sample was removed as the number of sequences was <1500). In order to explore the impact of the different supplementations/treatments on the overall structure of the mice's microbiota, permutational multivariate analysis of variance using Bray-Curtis distance (ADONIS) at the ASV level was performed using phyloseq package including the CC, antibiotic, and selenium supplementation as independent variables. The visualization of the beta diversity of the microbial communities was assessed by Principal Coordinates Analysis (PCoA) and Canonical Correspondence Analysis (CCA) on the total sum transformed data. To decipher the potential effect of the treatments in specific taxa from the microbiota composition, initial taxonomical taxa were filtered, and those taxa present < 3 times in at least 20% of the samples were removed from the compositional analysis. Differences between groups were evaluated by the Linear Discriminant Analysis Effect Size (LEfSe) by the microbiomeMarker package (Leo Lahti, 2017) using LDA> 3 and FDR> 0.2 as thresholds for significance. Furthermore, differences between groups were also assessed by the Wilcoxon test on the centered log-ratio (CLR) transformed data with multiple test corrections through the False Discovery test Rate (FDR) (FDR<0.2 was considered significant) (Fig. 1).

3. Results

3.1. Impact of the exposure to the "Chemical Cocktail" on mice plasma selenoproteome: the role of selenium supplementation and microbiota depletion

The typical distribution patterns of selenoproteins in plasma present the majority of Se accounted by SELENOP, followed by GPx, SeAlb, and

frequently, undetectable concentrations of selenometabolites, which eluted in a single peak after GPx (García-Sevillano et al., 2014c) This order in the Se distribution of plasma selenoproteins is the typical one for mice plasma, but the concentrations of selenoproteins changed between the different groups. Fig. 2 shows the typical mass flow superimposed chromatograms of conventional and antibiotic-treated mice exposed to the CC fed Se-supplemented or regular rodent diets, using the approach 2D-SEC-AF-ICP-MS. One-way ANOVA analysis was carried out to determine statistically significant differences in the concentration of selenoproteins and the total Se content in the five experimental groups C, CC, CC-Se, CC-Abx, and CC-Abx-Se. The fold changes (FC) of selenoproteins concentrations from different groups (Table 1) were calculated to check if Se-supplementation (groups CC-Se and CC-Abx-Se) shapes the plasma mice selenoproteome and modifies the total Se content in conventional and microbiota depleted mice exposed to the CC. Table 1 shows the averaged concentration of Se in different selenoproteins, the total Se content, and their fold changes in mice plasma. Our results (Table 1) showed that the exposure of conventional mice fed a regular rodent diet to the CC, slightly increased plasma GPx (CC/C>1), while the concentration of SELENOP and especially that of SeAlb, decreased after the exposure (CC/C<1). In conventional mice fed a Se-supplemented diet exposed to the CC, results showed that Se reduced the concentration of GPx in plasma mice (CC-Se/C<1) at lower levels than in the control, but the concentrations of SELENOP and SeAlb were also decreased (CC-Se/C<1). In relation to the microbiota-depleted mice model (Abx), results showed the absence of significant changes in mice plasma selenoproteome related to Se-supplementation against the
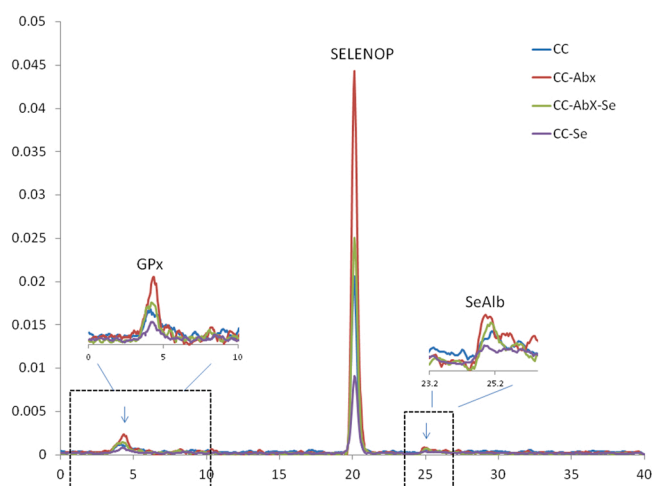

Fig. 2. Mass flow chromatograms obtained by 2D-SEC-AF-ICP-MS corresponding to control mice and conventional mice exposed to CC in the different groups.
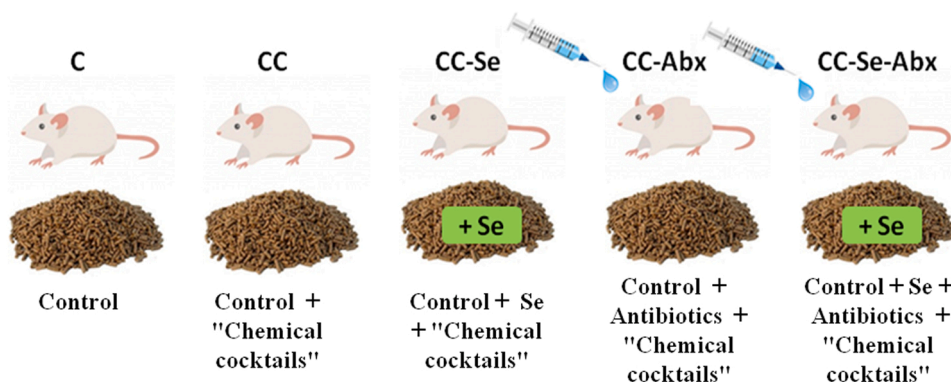

Fig. 1. Experimental design showing the studied groups.

Table 1
Averaged concentration of selenium in selenoproteins, total selenium and fold changes.

Selenoproteins Concentration (ng Se per g of plasma) ± S.E.M (n = 10 mice per group)					
Groups	GPx	Se metabolites	SELENOP	SeAlb	Total Se
C	15.2 ± 1.6	<LOD	381.4 ± 11.2	28.1 ± 2.2	424.7 ± 14.3
CC	16.5 ± 0.7	<LOD	100.5 ± 2.4	1.9 ± 0.8	120.9 ± 1.5
CC-Se	12.4 ± 1.3	<LOD	77.8 ± 2.1	3.3 ± 0.7	94.5 ± 1.7
CC-Abx	22.1 ± 1.1	<LOD	186.5 ± 5.3	36.4 ± 1.5	247.9 ± 10.4
CC-Abx-Se	27.9 ± 1.7	<LOD	151.3 ± 2.7	14.6 ± 0.8	199.2 ± 3.5
Fold changes					
Groups	GPx	Se metabolites	SELENOP	SeAlb	Total Se
CC/C	**1.07 (p = 0.05)**	–	**0.26 (p = 0.003)**	**0.07 (p = 0.000)**	**0.28 (p = 0.000)**
CC-Se/C	**0.81 (p = 0.05)**	<LOD	**0.20 (p = 0.001)**	**0.12 (p = 0.000)**	**0.22 (p = 0.003**
CC-Abx/C	**1.43 (p = 0.01)**	<LOD	**0.49 (p = 0.000)**	1.31 (p > 0.05)	**0.58 (p = 0.003)**
CC-Abx-Se/C	**1.81 (p = 0.023)**	<LOD	**0.40 (p = 0.000)**	**0.53 (p = 0.017)**	**0.47 (p = 0.000)**
CC-Abx-Se/CC-Abx	1.26 (p > 0.05)	<LOD	0.81 (p > 0.05)	0.40 (p > 0.05)	0.80 (p > 0.05)

LOD: Limit of Detection of selenometabolites 0.5 ng g-1; p: p-value from ANOVA followed by Tukey Test (only significant p-values are shown in the table).

exposure to the CC, since the fold changes CC-Abx-Se/CC-Abx were not significant for any selenoprotein. As in the case of conventional mice, the exposure to the CC in microbiota-depleted mice showed an increase in plasma GPx and a decrease in SELENOP, but not in SeAlb. Regarding the sense of the fold change, the joint effect of Se-supplementation and microbiota-depletion in microbiota depleted mice, induced the same changes in mice plasma selenoproteome as when conventional mice were exposed to the CC (CC-Abx-Se/C vs CC/C).

3.2. Arsenic metabolism in mice plasma

The main species in control mice plasma are DMA followed by MA. Inorganic arsenic and AB were absent in all the analyzed samples. Fig. 3 shows a typical AE-ICP-MS superimposed chromatogram of As speciation in plasma mice exposed to the CC-fed Se-supplemented and regular rodent diets. Table 2 shows the concentration of As species in mice plasma samples of the different groups of regular rodents. Table 2 shows that DMA and especially MA increased after exposure to the CC (CC/C>1). However, Se-supplementation ameliorated this effect (CC-Se/C vs CC/C), especially for MA, which reached lower levels than in the control (CC-Se/C<1). Regarding the microbiota-depleted mice model, Se-supplementation also ameliorated the increase of DMA and, to a higher extent, MA induced by the CC (CC-Abx-Se/C vs CC/C). Microbiota depletion also ameliorated the increase of DMA and MA induced by the CC and there were no significant differences between both, Se-supplementation and microbiota depletion (CC-Abx-Se/CC-Abx,

Fig. 3. AE-ICP-MS chromatograms of arsenic species were obtained from the plasma of conventional mice exposed to CC in the different groups.

p > 0.05). Besides this significant alteration of the As speciation profile in mice plasma after Se-supplementation, the levels of iAs were also altered. Total As increased after CC exposure and also, Se-supplementation and microbiota depletion ameliorated this effect and to a similar extent (FC 1.16 vs 1.33, respectively).

3.3. Plasma mice metabolome and the role of selenium supplementation and microbiota depletion

Different species of amino acids, monoacylglyceride compounds, and monosaccharides showed significant variations in all groups compared with the control. Metabolites with statistically significant differences among the groups versus the control are shown in Table (S2). PCA plots showed a good clustering of the QCs samples (Fig. S1). Moreover, co-efficients of variation (CV) of QCs were calculated (Table S3), and only those metabolites with CV lower than 20% were considered. Fig. 4 shows the PLS-DA obtained by GC-MS comparing mice plasma metabolomes pairwise (top) and all the groups under study (bottom). As we can see, the separation between groups was possible in all pairwise comparisons, except in the case of the antibiotic-treated mice model exposed to CC when compared with mice fed a Se-supplemented diet and regular rodent diet. Moreover, Table S4 shows the values of R^2 and Q^2 of the PLS-DA score plot in all models and Fig. S2 shows the metabolomic profiles from GC-MS analysis. Fig. 5 shows a heatmap diagram with the abundance of the most significant metabolites in C, CC, CC-Se, CC-Abx, and CC-Abx-Se mice groups compared with the C mice group. The most impaired classes of compounds found in the groups under study were eight compounds (Fig. 5 and Table S2). The plots demonstrated that conventional mice fed a regular rodent diet presented lower abundance in all the metabolites after CC exposure (CC vs C), especially for glucose (0.29-fold) and 1-monopalmitin (0.21-fold). Interestingly, these metabolites increased after Se-supplementation to higher levels than in the control group. On the other hand, as can be seen in Fig. 5, there are two areas of metabolites that can be differentiated in conventional mice exposed to the CC-fed regular rodent diet or supplemented with Se (CC-Se vs CC). Thus, we can observe after Se-supplementation an increased abundance (red color) of 1-monopalmitin (1.34-fold) and glucose (1.78-fold) and decreased levels (blue color) of the other six metabolites (Table S3). We also found the dysregulation of five metabolites in antibiotic treated-mice fed regular diet exposed to the CC group compared with mice fed regular diet exposed to the CC (CC-Abx vs CC), such as glucose, 1-monopalmitin, gluconic acid, threonic acid, and tyrosine. In this sense, 1-monopalmitin, glucose, threonic acid, and gluconic acid were the most affected compounds, with a significantly increased in 1-monopalamitin (1.87-fold), glucose (1.75-fold), and threonic acid (1.84-fold) while a decreased in gluconic
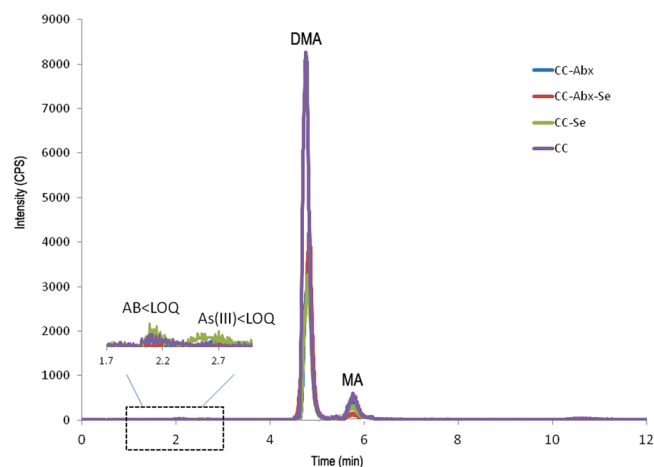
Table 2

Averaged concentration of arsenic species in mice plasma and fold changes between groups.

Arsenic species										
Concentration (ng As per g of plasma) ± S.E.M (n = 10 mice per group)										
	AB	iAs	MA			DMA			Total As as sum of species	SMI
C	<LOD	<LOD	2.6	±	0.8	20.8	±	0.7	23.4	8
CC	<LOD	<LOD	8.3	±	0.7	48.0	±	0.2	56.3	6
CC-Se	<LOD	<LOD	2.3	±	0.4	28.8	±	0.4	31.1	13
CC-Abx	<LOD	<LOD	2.2	±	0.2	24.8	±	0.2	27.0	11
CC-Abx-Se	<LOD	<LOD	2.7	±	1.4	26.0	±	0.3	28.7	10
Fold changes										
	MA	DMA	AB	iAs		Total As				
CC/C	**3.21(p = 0.001)**	**2.31(p<0.002)**	–	–		**2.41(p = 0.003)**				
CC-Se/C	**0.82(p = 0.05)**	**1.39(p<0.002)**	–	–		**1.33(p = 0.001)**				
CC-Abx/C	0.77(p > 0.05)	**1.19(p<0.019)**	–	–		**1.16(p = 0.011)**				
CC-Abx-Se/C	**1.03(p = 0.05)**	**1.25(p<0.021)**	–	–		**1.23(p = 0.018)**				
CC-Abx-Se/CC-Abx	0.34(p > 0.05)	1.05(p > 0.05)	–	–		1.06(p > 0.05)				

iAs: inorganic arsenic (sum of As (III) and As(V)). LOD and LOQ of As (Table S1); p: p-value from ANOVA followed by Tukey Test (only significant p-values are shown in the table). SMI: secondary methylation index (DMA/MA).
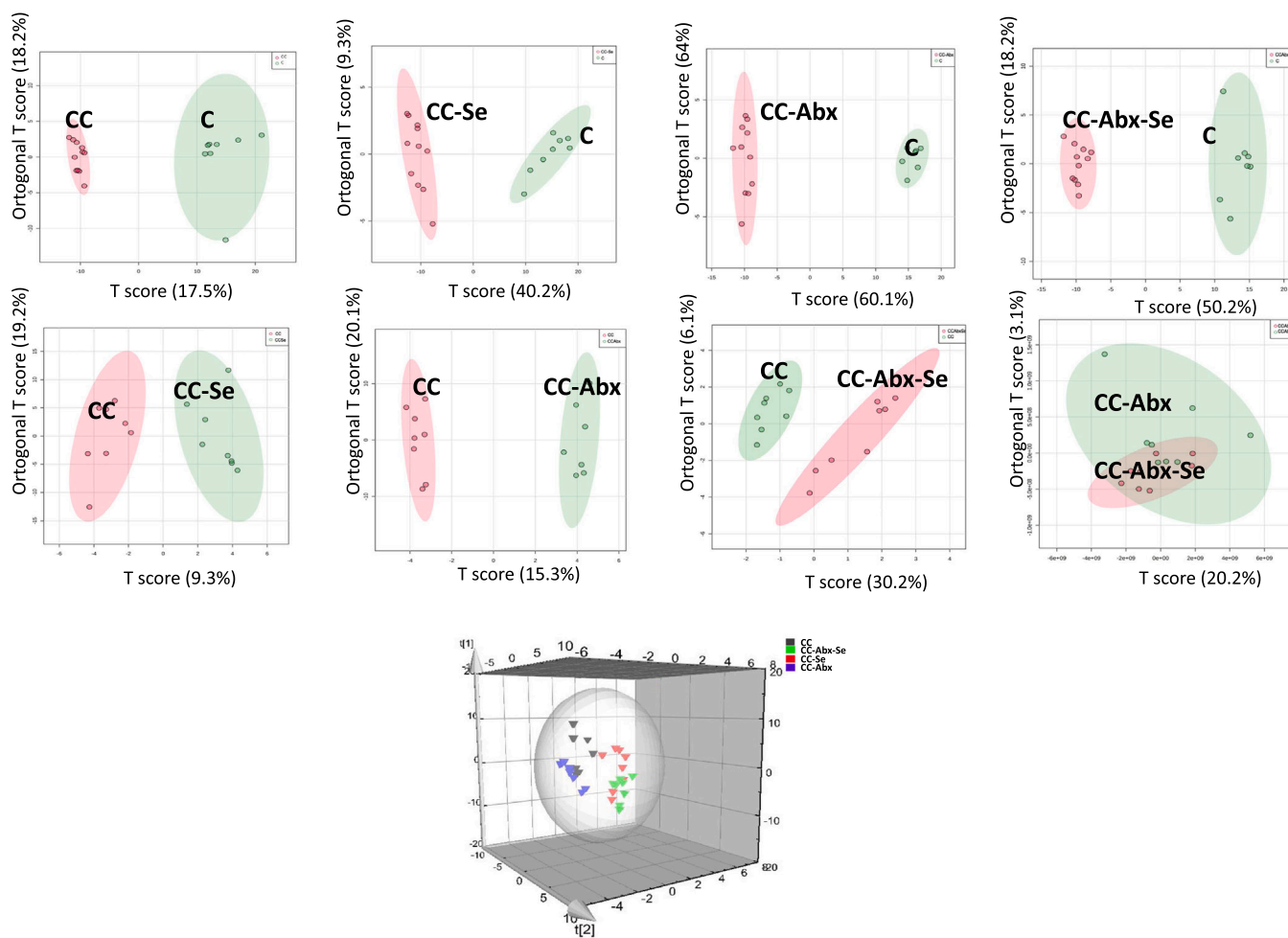

Fig. 4. PLS-DA obtained was showing the comparison of all the metabolites detected in mice plasma from the different groups under study.

acid (0.47-fold) (TableS2). The highest number of altered compounds (7 metabolites) was found in antibiotic treated-mice fed Se supplemented diet exposed to the CC compared to mice fed regular diet exposed to the CC (CC-Abx-Se vs CC). In principle, stearic acid was significantly increased (8.78-fold) and the results also showed a significant increase in 1-monopalmitin (1.46-fold) and glucose (1.70-fold). In the microbiota-depleted mice model, unlike the rest of the mice groups, tyrosine was significantly altered when compared with mice exposed to

the CC-fed regular rodent diet (CC-Abx vs CC; CC-Abx-Se vs CC) (TableS2). On the other hand, the pathway analysis showed a total of 10 impaired routes including 25 metabolisms in different groups when compared with the control. Fig. 6 shows the diagram of the pathway analysis, and Table S5 describes the numbers of hits, s-values, and the impact of the affected metabolic routes by the altered metabolites found in CC, CC-Se, CC-Abx, and CC-Abx-Se groups. As can be seen in Fig. 6A, the exposure to the CC in conventional mice significantly altered the
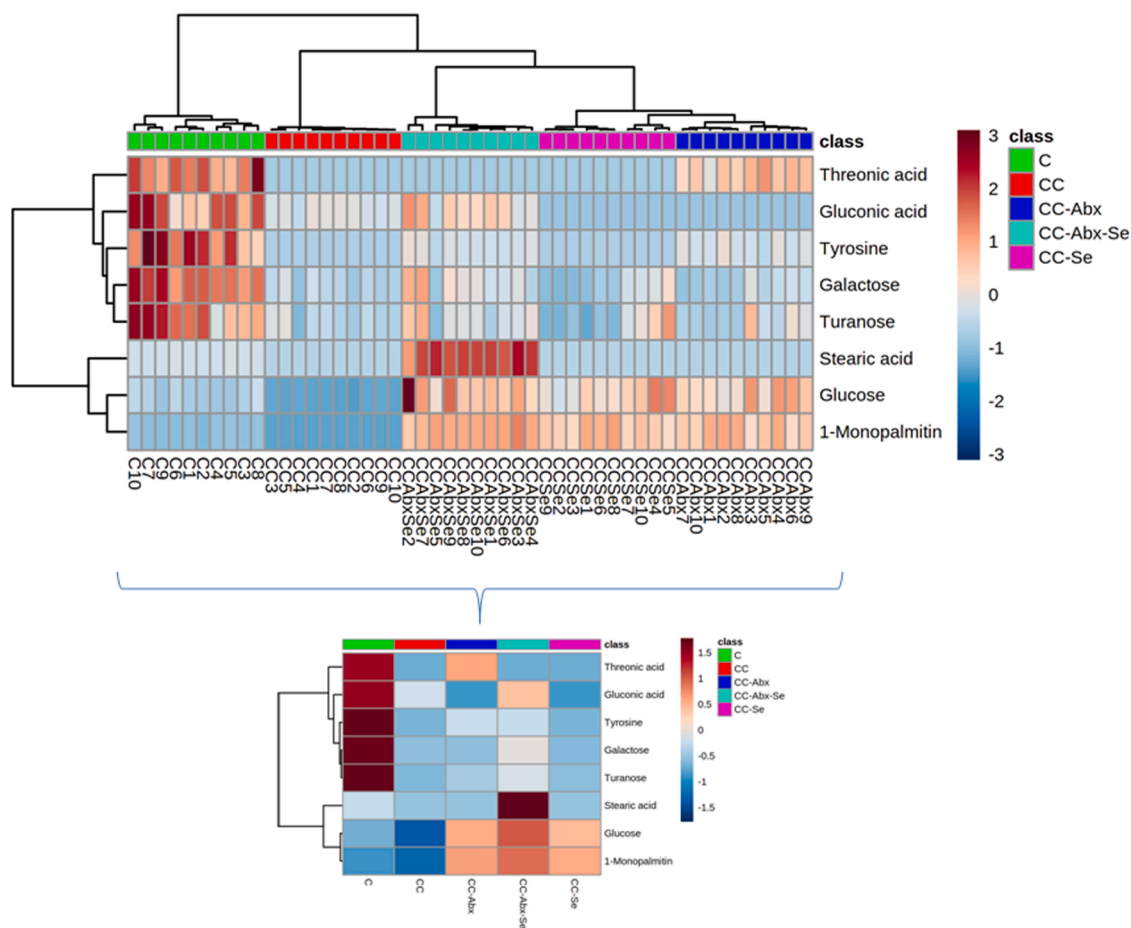
Fig. 5. Cluster heatmap showing the abundance of plasma metabolites annotated in individual samples (top) and averaged for each mice group (bottom): C, CC, CC-Se, CC-Abx, CC-Abx-Se.

pentose phosphate, galactose, and glycolysis/gluconeogenesis pathways, but after Se-supplementation (Fig. 6B), pentose phosphate pathway impairment disappeared. As can be shown, in microbiota-depleted mice models, the changes were less evident after Se-supplementation, but we can highlight that the depleted microbiota causes disorders in tyrosin metabolism affected in metabolic routes of phenylalanine, tyrosine, and tryptophan biosynthesis.

3.4. Impact of the chemical cocktail exposure, selenium supplementation and microbiota depletion on the gut microbiota

Both gut microbiota composition and diversity were affected by the administration of CC, antibiotics, and Se-supplementation in mice (Fig. 7). In terms of alpha diversity, the treatments significantly impact microbial richness (Chao index, $p < 0.001$) with differences among groups. Antibiotic treated mice showed a lower Chao index compared to the C group (C vs CC-Abx, $p = 0.002$) while no differences were observed in the CC-Se group (C vs CC-Se, $p = 0.089$). The CC-Abx-Se group showed significantly lower microbial richness and diversity than the rest of the groups ($p < 0.05$) (Fig. 7A).

Regarding beta-diversity, the Adonis test based on Bray-Curtis distance showed differences between analyzed groups ($R^2 = 0.350$, F = 5.034, $p = 0.001$) as can be observed in the PCoA (Fig. 7B). When the three treatments were analyzed independently, CC ($R2 = 0.100$, $p = 0.001$), antibiotics ($R2 = 0.073$, $p = 0.001$), and Se supplementation ($R2 = 0.033$, $p = 0.001$) showed a significant impact on the overall microbiota structure. Furthermore, canonical correspondence analysis (CCA) showed the significant clustering of conventional mice groups according to the treatments highlighting the differences in microbial

composition between groups (F=2.68, $p = 0.001$) (Fig. 7C). As can be observed in both PCoA and CCA plots, the Se-supplemented group after antibiotic treatment (Abx-Se) showed a fecal microbiota that resembled more the control group than the group with microbiota depletion (Abx). However, in the CC treated group, the Se supplementation after the antibiotic treatment (CC-Abx-Se) was not able to revert the effect of microbial depletion and the microbial profile of this group is different from the rest of the groups suggesting a great impact of the CC in the overall microbiota structure (Fig. 7 B, C).

Thus, conventional mice exposed to the CC-fed regular rodent diet (CC) are well separated from mice fed Se-supplemented diet (CC-Se) and to the control (C). Regarding the mice model with microbiota-depleted by antibiotics, we observed two clusters corresponding to microbiota depleted mice (Abx) and a mixture between the Abx mice model exposed to CC fed the Se-supplemented diet and regular rodent diet (Se-Abx-CC and Abx-CC). Differences in microbiota composition were assessed by LEfSe analysis (Fig. 8) and Mann-Whitney test on CLR transformed data (Table S6). At the phylum level, all the most relatively abundant phyla showed significant differences between groups (Fig. 8D, Table S6). While all the groups treated with CC showed a diminished relative abundance in the Actinobacteria phylum, especially those with a depleted microbiota (CC-Abx), in the CC-Abx-Se group the levels of this phylum were recovered compared to the non-depleted group (CC). At the genus level, Lefse analysis was used to compare groups by pairs of groups to explore the effect of each specific treatment. Regarding the effect of CC, regular-fed mice were enriched in groups from the Lachnospiraceae family and *Eubacterium* genus while the CC group is characterized by Bacteroidetes genera such as *Bacteroides* and *Alloprevotella* (Fig. 8A). Interestingly, in the microbiota-depleted group exposed to the
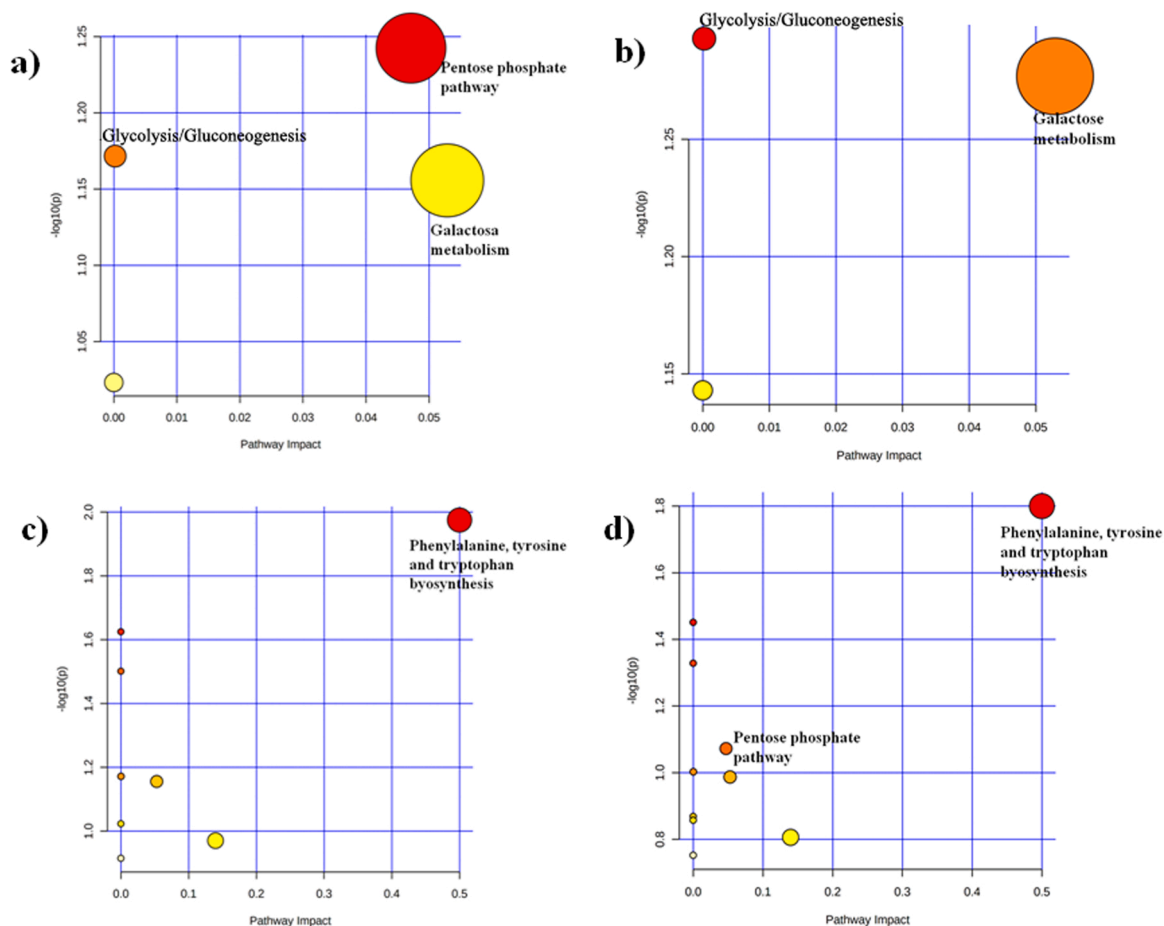
Fig. 6. Pathway analysis plots indicating the most affected metabolic routes in CC (a), CC-Se (b), CC-Abx ©, and CC-Abx-Se (d) groups against C. The *p*-value (indicated by a color gradient: from white (highest p-value) to red (lowest p-value)) is the *p* calculated from the enrichment analysis, and the impact (indicated by dot size) is the pathway impact value calculated from the pathway topology analysis.

CC (CC-Abx) some of the representative taxa are the same that characterized C mice, such as the mentioned Lachnospiraceae and *Eubacterium* groups suggesting a potential interaction between the antibiotic and CC treatments (Fig. 8B). Similar to what was observed in the alpha and beta diversity analysis, the microbiota composition of the CC-Abx-Se mice was greatly impacted by the convention of the treatments showing a microbial biomarker completely different than the CC-Abx and CC groups (Fig. 8C, D; respectively). As can be observed, these groups showed enrichment of *Clostridium innocuum* group, *Escherichia/Shigella*, and *Akkermansia* genera.

3.5. Associations between gut microbiota and plasma selenoproteome

Specific relations between plasma selenoproteome and gut microbiota composition were found in groups C, CC, CC-Se, CC-Abx, and CC-Abx-Se, specifically at the genus level (Table S7, Fig. 9). It is noteworthy that microbiota-depleted mice fed a regular rodent diet (CC-Abx) presented the highest number of associations between gut microbiota and selenoproteins, while the Se-supplemented group presented the lowest (CC-Abx-Se). This last fact could be explained by the reduction of the diversity in the group. Thus, the number of correlations follows the order: CC-Abx-Se<C<CC<CC-Se<CC-Abx. Remarkably, as can be seen in Fig. 9, Se-supplementation changed and increased the associations between selenoproteins and gut microbiota at the genus level. In conventional mice exposed to the CC fed regular rodent diet (CC), the selenoprotein which correlated with the highest number of genera is GPx (6 significant and positive associations) is GPx, followed by SeAlb (2 significant correlations, positive and negative) and total Se (2 significant

positive correlations), while SELENOP does not correlate with any selenoprotein. After Se-supplementation (CC-Se), the number of correlations increased, and GPx significantly correlated with 8 different genera (2 positives), SeAlb with 3 (2 positives), SELENOP with 1 (negative), and total Se with 4 (2 positives).

In the CC-Abx-Se, only SeAlb correlated negatively with *Parabacteroides* (rho=−0.773, *p* = 0.024) and *Oscillospiraceae UCG-003* (rho=−0.796, *p* = 0.018) in CC-Abx-Se group. In CC-Se group, the concentration in plasma of GPx correlated negatively with the abundance of *Lachnospiraceae NK4A136 group* (rho=−0.663, *p* = 0.037), *Roseburia* (rho=−0.632, *p* = 0.05), *Anaeroplasma* (rho=−0.713, *p* = 0.0021) *and Butyricicoccus* (rho=−0.638, *p* = 0.047) and positively with *Lactobacillus* (rho=0.632, *p* = 0.05) and *Streptococcus* (rho=0.693, *p* = 0.047). In this group (CC-Se), the concentration of SELENOP in plasma only correlated with the abundance of *Mucispirillum* (rho=−0.709, *p* = 0.022), while SeAlb was associated to the abundance of *Muribaculum* (rho=0.707, *p* = 0.022), *Parabacteroides* (rho=−0.616, *p* = 0.058) and *Bilophila* (rho=−0.744, *p* = 0.014).

4. Discussion

Our results from chemical speciation of selenoproteins and arsenic in plasma, plasma metabolomics and gut microbiota profiling, reveals that in general, Se-supplementation impact significantly on conventional mice (CC-Se), but it is limited in the microbiota depleted mice model (CC-Abx-Se) (Fig. S3). Our previous works about Se-supplementation in both mice models (Callejón-Leblic et al., 2021; D'Amato et al., 2020), but without exposure to the CC, pointed out that Se-supplementation
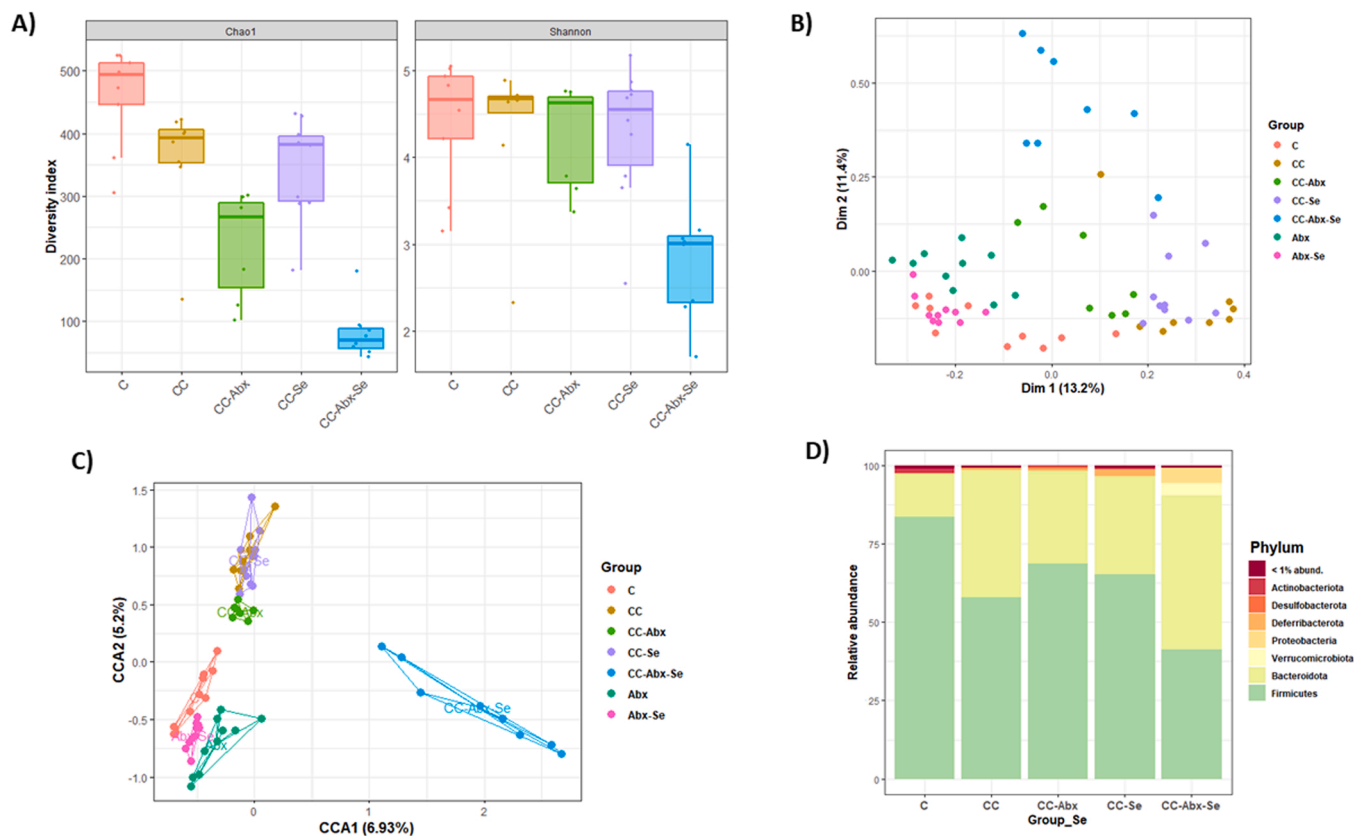
Fig. 7. Effect of chemical cocktails, antibiotic treatment, and selenium supplementation on the microbiota of conventional mice. A) Boxplots showing differences in alpha diversity of the fecal microbial communities according to groups measured as richness (Chao1) and diversity (Shannon) indexes. B) Principal Coordinate Analysis (PCoA) of microbial beta-diversity based on the Bray Curtis distance (R2 =0.350, F=5.034, p = 0.001). C) Canonical correspondence analysis (CCA) showing the clustering of the mice according to the differences in microbiota composition among groups (F=2.68, p-value=0.001). D) Bar plots showing the microbiota composition at phylum level in relative abundance according to groups.

significantly modulated gut metabolome (D'Amato et al., 2020), gut microbiota, plasma selenoproteome and plasma metal homehostasis (Callejón-Leblic et al., 2021) in both mice models. Thus, herein the discussion is focused in the CC-Se group where results clearly suggest an intertwined mechanism between selenoproteins and gut microbiota.

4.1. Mice plasma selenoproteome

All the analyzed mice plasma samples present the same typical profile for humans and mice in which SELENOP accounts for the highest content of Se (>50% of total Se) followed by GPx (~15–20% of total Se) and SeAlb (~15–20%) (Callejón-Leblic et al., 2021; Mostert, 2000; Busto et al., 2016). Thus, these three selenoproteins account for most of Se in plasma and are the commonly used biomarkers to assess Se status in human serum and plasma (Busto et al., 2016). Plasma selenoproteomes were significantly altered after the exposure of conventional mice to the CC. Likewise, as the concentration of plasma GPx increased after the exposure, it could be related with an increase of the oxidative stress induced by the pollutants, since the main role of GPx is as an antioxidant (Björnstedt et al., 1994). Otherwise, the main roles of SELENOP and SeAlb are the transport of Se (Saito, 2021; Suzuki et al., 2013) and thus, the decreased concentrations in mice plasma after the exposure may indicate the transport of Se to organs prone to damage. In addition, Se-supplementation decreased the concentration of plasma GPx to levels below the control, which could be related by its antioxidant action. Moreover, although the concentrations of SELENOP and SeAlb also decreased in plasma after the exposure in mice fed Se-supplemented diet when compared to control mice, the change was significantly less in magnitude for SeAlb than in the case of mice fed

regular rodent diet.

As Se-supplementation did not change mice plasma selenoproteome in microbiota depleted mice exposed to the CC, an intertwined mechanism between Se, selenoproteins and gut microbiota is suspected. Our previous work (Callejón-Leblic et al., 2021), demonstrated that Se-supplementation modulated the concentration of the antioxidant GPx and the Se-transporter SeAlb in mice plasma (not exposed to the CC) as well as the metal homeostasis, being influenced by microbiota disruption, also suggesting an intertwined mechanism.

4.2. Mice plasma arsenic species

As is mainly metabolized in the liver and excreted in the urine after methylation and accumulated in skin, nails and hair (Rasheed et al., 2019). The classical metabolic pathway of As is generally accepted to proceed by oxidative methylation and repetitive reduction (Hayakawa et al., 2005). In the majority of mammalian species, iAs is methylated to MA and DMA that are more quickly excreted by urine than iAs, especially the trivalent form (arsenite, As^{III}), which is highly reactive with tissue components (Vahter, 1999) Our results demonstrated that iAs is absent in mice plasma in all the analyzed samples and only methylated species were detected, which may indicate the methylation of As to be further excreted by urine. As expected, the exposure to the CC increased plasma mice As concentrations, but Se-supplementation ameliorated this effect. Interestingly, the absence of gut microbes also decreased As concentration in mice plasma. Moreover, in the conventional mice model exposed to the CC, the DMA/MA ratio increased from 6 (mice fed regular rodent diet) to 13 (mice fed Se-supplemented diet), that could be related with an increased methylation for urine excretion
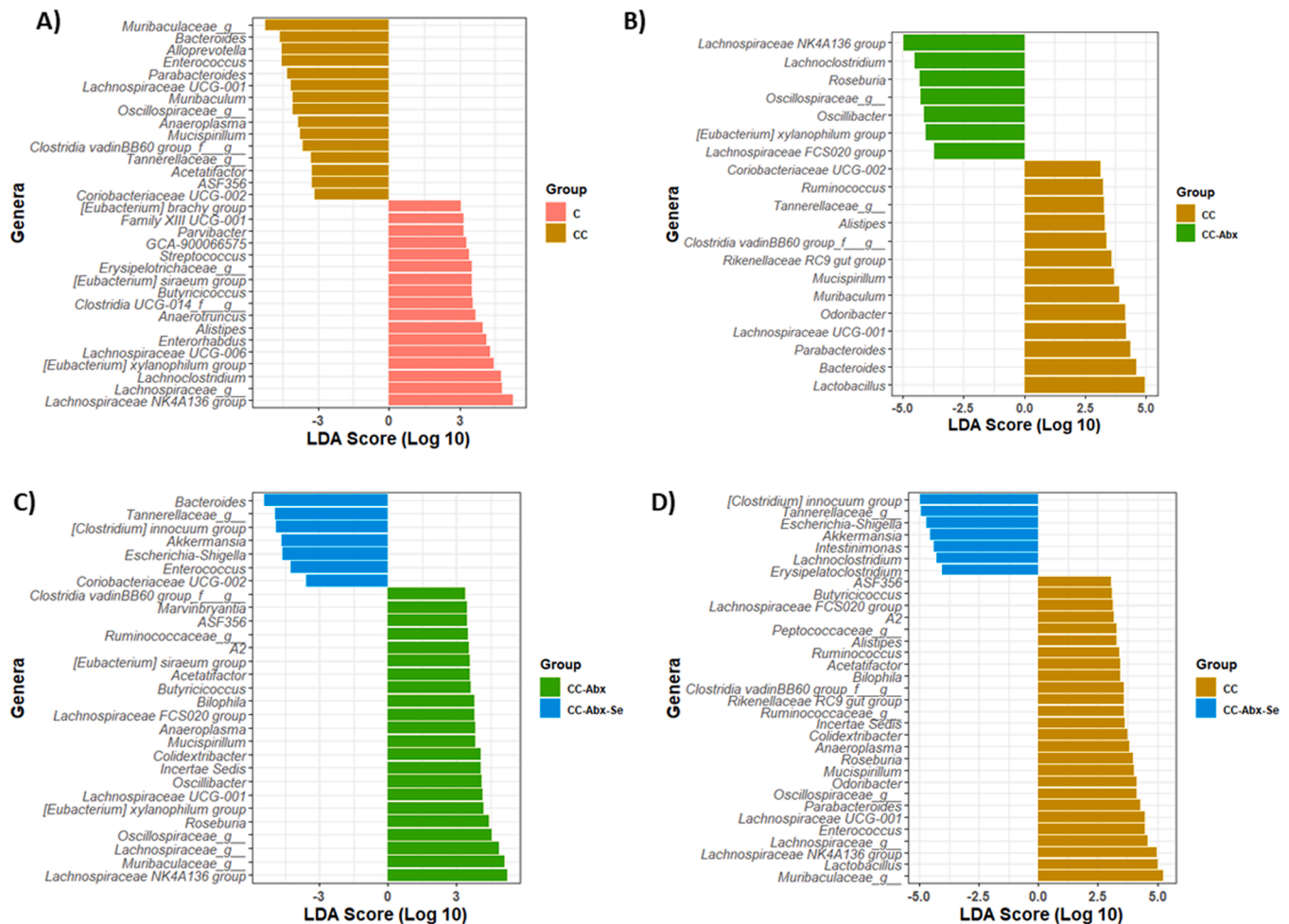
Fig. 8. Differences in gut microbiota composition between groups according to mice treatment. Linear Discriminant Analysis Effect Size (LEfSe) plot of taxonomic biomarkers that characterize the gut microbiota of the different groups at the genus level. A threshold of 3 was considered for the logarithmic discriminant analysis (LDA) and only those taxa with an FDR > 0.2 were included in the plot.

(Torres-Sánchez et al., 2016). This index did not change in microbiota depleted mice models.

4.3. Mice plasma metabolome

The exposure to the CC significantly impaired mice 'plasma metabolome. As shown in Fig. 5, gluconic acid, glucose, galactose and turanose decreased significantly after the exposure to the CC. Intermediate metabolites in energy metabolism such as glucose have been reported to be depleted under inorganic arsenic exposure due to perturbations in carbohydrate metabolism (García-Sevillano et al., 2014a; Reichl et al., 1988, 1989; Szinicz and Forth, 1988). Studies also showed that As and Cd alter the activity of several enzymes related with glycolysis, glucogenesis, pentose phosphate pathway and gluconeogenesis (Hu et al., 2012).

According to these results, the pathway analysis showed that the pentose phosphate pathway was one of the most affected metabolic routes by the exposure of CC and Se-supplementation (CC-Se) (Fig. 6 A, B). This fact can be explained because the Se-supplementation can restore the glycemic control, largely by modifying the activities of glycolytic and gluconeogenic enzymes and improving insulin sensitivity that has been previously altered by the exposure to the CC (Pepper et al., 2011). On the other hand, the pathway analysis also revealed impairments in tyrosine, tryptophan and phenylalanine metabolism in CC-Abx and CC-Abx-Se groups (Fig. 6C, D). Gut microbiota induced shifts in the levels of these amino acids, mainly tryptophan, have been related to

alterations in the function of the central and enteric nervous systems (Callejón-Leblic et al., 2022; Kaur et al., 2019).

4.4. Mice gut microbiota and the associations with plasma selenoproteome

Se-supplementation induced changes in mice gut bacterial beta-diversity exposed to the CC, but only in conventional mice. In a previous work, our results showed that Se-supplementation modulated gut microbiota diversity and richness, especially in microbiota depleted mice (Callejón-Leblic et al., 2021). However, this work demonstrated that this is not possible in the case of mice exposed to the CC as the joint effect of Abx and CC exposure limited the action of Se-supplementation. Also, previous results demonstrated that Se increased the relative abundance of some health relevant taxa (e.g., *Lactobacillus* genus and families *Ruminococcaceae* and *Christensenellaceae*) (Callejón-Leblic et al., 2021). In this work, the CC group was enriched in groups from the Lachnospiraceae family and *Eubacterium* genus compared to CC-Se group which was characterized by *Bacteroides* and *Alloprevotella* genera. *Eubacterium limosum* has been reported to be capable of O-demethylation of pollutants toward O-methylated isoflavones (Yim et al., 2008), while *Alloprevotella* has been related with neuronal synapse (Balaguer-Trias et al., 2022). Moreover, Lachnospiraceae and *Eubacterium* taxa were enriched in both CC-Abx and C groups, while most altered group (CC-Abx-Se) was characterized by *Clostridium innocuum* group and *Escherichia/Shigella* genus suggesting a synergic effect of the
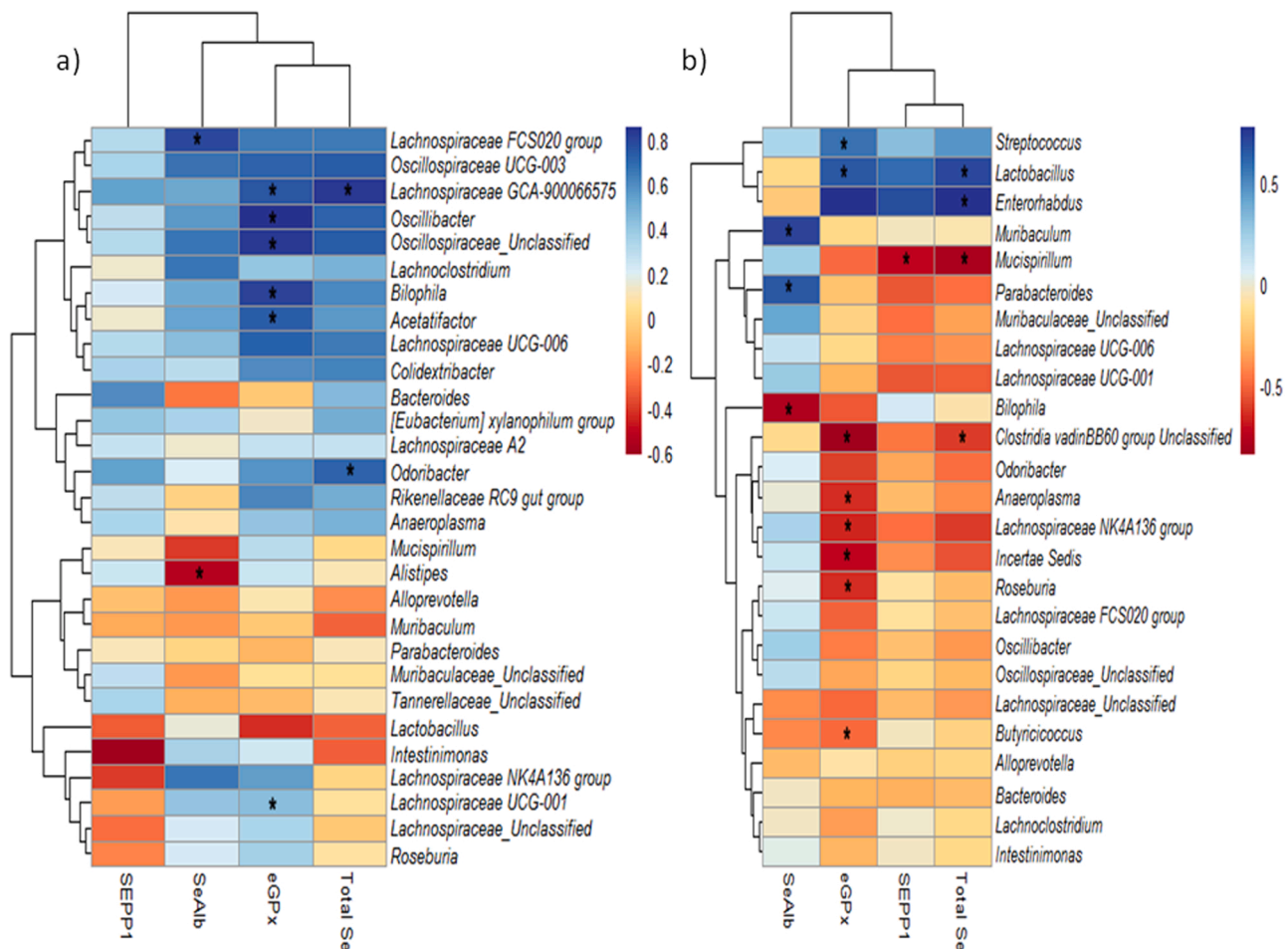
Fig. 9. Spearman correlation matrix heatmaps for plasma selenoproteins and microbiota at genus level in a) CC group, b) CC-Se group.

CC and the Abx which would interfere in the potential effect of the Se as microbiota modulator. *Clostridium innocuum* is a vancomycin-resistant pathogen that might cause diarrhea related to antibiotics (Chia et al., 2018). Further studies are needed to evaluate the molecular mechanisms that play a role in the relation between Se-supplementation and microbiota composition and how some other chemical substances would interfere in this effect through an alteration in the microbial populations. It would be especially relevant to decipher the interaction between the antibiotic-related shift in gut microbiota and the potential diminished effect of the analyzed CC since it could reveal the crucial role of microbiota in the physiological response to other chemical exposures.

Regarding the associations between plasma selenoproteins and gut microbiota in the CC-Se group, the concentration in plasma of GPx was negatively correlated with the abundance of *Lachnospiraceae NK4A136 group* and positively with *Lactobacillus*, both considered potential probiotic groups (Wu et al., 2021; Reid, 1999). GPx was also negatively associated with *Roseburia, Anaeroplasma and Butyricicoccus* and positively with Streptococcus. It has been previously reported that correct levels of *Roseburia* ameliorates depressive-like behaviors by the regulation of inflammation through the gut-brain axis (Xu et al., 2021), while several brain metabolites were positively associated with the abundance of *Anaeroplasma* (Nguyen et al., 2019), a genus which elicited various host immune responses in a wide number of human diseases such as colon cancer (Yang et al., 2012; Xu et al., 2013). *Butyricicoccus* has been previously related with stress-induced depressive-like behavior (Tian et al., 2019a).

In this group (CC-Se), plasma SELENOP was negatively associated with *Mucispirillum*. A positive association has been described between the abundance of *Mucispirillum* and testosterone and sperm activity in

Lactobacillus plantarum TW1–1 supplemented mice (Tian et al., 2019b) as well as with testicular selenoproteome (Ramírez-Acosta et al., 2022). A decrease in the level of this genus in mice fed supranutritional Se has been previously reported (Zhai et al., 2018). Finally, SeAlb was associated with *Muribaculum*, which decreases in a regular rodent model of Crohn's disease (Dobranowski et al., 2019), *Parabacteroides*, a gamma-aminobutyric acid (GABA)-producing bacterial genus (Ezeji et al., 2021) and *Bilophila*, that has been isolated from several clinical specimens (Baron et al., 1992).

5. Conclusions

The analytical platform based on metallomics, metabolomics, and metataxonomics is a powerful tool to have a holistic view of the impact of pollutants. At molecular levels, CC exposure increased the antioxidant glutathione peroxidase in plasma and decreased the transporters selenoprotein P and selenoalbumin, while Se-supplementation decreased glutathione peroxidase below those in control conventional mice, but not in Abx. Se-supplementation increased the As methylation rate, possibly favoring its excretion. Also, the absence of gut microbes decreased As in plasma. Moreover, plasma metabolomes differ in all pairwise comparisons, except in Abx when comparing mice fed Se-supplemented diet and regular rodent diet, suggesting that, Se required the presence of gut microbiota to induce metabolic changes. Regarding gut microbiota profiles, the potential antagonistic role of Se-supplementation against CC and Abx changed in Se-CC-Abx that present the most altered gut microbiota suggesting a synergism. Also, Abx and CC altered gut microbiota, but the joint effect of Abx-CC revealed the enrichment of several taxa found in the control group.

Our results suggest numerous interactions between chemicals mediated by gut microbiota including the potential beneficial role of Se-supplementation. In addition, the effects of pollutants cannot be studied in isolation due to the presence of joint effects. However, the precise links need to be ascertained and further studies targeted to the specific mechanisms are needed.

Funding Sources

CRediT authorship contribution statement

A. Arias-Borrego: Methodology, Formal analysis, Data curation, Investigation, Writing – original draft, Writing – review & editing. **M. Selma-Royo**: Investigation, Methodology, Writing – review & editing. **M.C. Collado**: Conceptualization, Methodology, Writing – original draft, Writing – review & editing. **N. Abril**: Conceptualization, Formal analysis, Investigation, Methodology, Writing – original draft, Writing – review & editing. **T. García-Barrera**: Conceptualization, Supervision, Methodology, Writing – original draft, Writing – review & editing, Funding acquisition, Project administration.

Author Contributions

The manuscript was written through contributions of all authors. All authors have given approval to the final version of the manuscript.

Declaration of Competing Interest

The authors declare that they have no known competing financial interests or personal relationships that could have appeared to influence the work reported in this paper.

Appendix A. Supporting information

Supplementary data associated with this article can be found in the online version at doi:10.1016/j.jhazmat.2022.129444.

References

Andy, M.K., 2008. An Introduction to dplR. Ind. Commer. Train. 10, 11–18.

Arias-Borrego, A., Velasco, I., Gómez-Ariza, J.L., García-Barrera, T., 2022. Iodine deficiency disturbs the metabolic profile and elemental composition of human breast milk. Food Chem. 371, 131329 https://doi.org/10.1016/J. FOODCHEM.2021.131329.

Balaguer-Trias, J., Deepika, D., Schuhmacher, M., Kumar, V., 2022. Impact of Contaminants on Microbiota: Linking the Gut–Brain Axis with Neurotoxicity. Int. J. Environ. Res. Public Health 19. https://doi.org/10.3390/ijerph19031368.

Baron, E.J., Curren, M., Henderson, G., Jousimies-Somer, H., Lee, K., Lechowitz, K., Strong, C.A., Summanen, P., Tuner, K., Finegold, S.M., 1992. Bilophila wadsworthia isolates from clinical specimens. J. Clin. Microbiol. 30, 1882–1884. https://doi.org/ 10.1128/jcm.30.7.1882-1884.1992.

Benramdane, L., Bressolle, F., Vallon, J.J., 1999. Arsenic speciation in humans and food products: A review. J. Chromatogr. Sci. 37, 330–344. https://doi.org/10.1093/ chromsci/37.9.330.

Beyrouty, P., Chan, H.M., 2006. Co-consumption of selenium and vitamin E altered the reproductive and developmental toxicity of methylmercury in rats. Neurotoxicol. Teratol. 28, 49–58. https://doi.org/10.1016/j.ntt.2005.11.002.

Björnstedt, M., Xue, J., Huang, W., Åkesson, B., Holmgren, A., 1994. The thioredoxin and glutaredoxin systems are efficient electron donors to human plasma glutathione peroxidase. J. Biol. Chem.

Busto, M.E.D.C., Oster, C., Cuello-Nuñez, S., Deitrich, C.L., Raab, A., Konopka, A., Lehmann, W.D., Goenaga-Infante, H., Fisicaro, P., 2016. Accurate quantification of selenoproteins in human plasma/serum by isotope dilution ICP-MS: Focus on selenoprotein P. J. Anal. . Spectrom. 31, 1904–1912. https://doi.org/10.1039/ c6ja00122j.

Callejón-Leblic, B., Selma-Royo, M., Collado, M.C., Abril, N., García-Barrera, T., 2021. Impact of Antibiotic-Induced Depletion of Gut Microbiota and Selenium Supplementation on Plasma Selenoproteome and Metal Homeostasis in a Mice Model. J. Agric. Food Chem. 69, 7652–7662. https://doi.org/10.1021/acs. jafc.1c02622.

Callejón-Leblic, B., Selma-Royo, M., Collado, M.C., Gómez-Ariza, J.L., Abril, N., García-Barrera, T., 2022. Untargeted Gut Metabolomics to Delve the Interplay between Selenium Supplementation and Gut Microbiota. J. Proteome Res. 21, 758–767. https://doi.org/10.1021/acs.jproteome.1c00411.

Chia, J.-H., Wu, T.-S., Wu, T.-L., Chen, C.-L., Chuang, C.-H., Su, L.-H., Chang, H.-J., Lu, C.-C., Kuo, A.-J., Lai, H.-C., Chiu, C.-H., 2018. Clostridium innocuum is a vancomycin-resistant pathogen that may cause antibiotic-associated diarrhoea. Clin. Microbiol. Infect. 24, 1195–1199. https://doi.org/10.1016/j.cmi.2018.02.015.

Choi, A.L., Budtz-Jørgensen, E., Jørgensen, P.J., Steuerwald, U., Debes, F., Weihe, P., Grandjean, P., 2008. Selenium as a potential protective factor against mercury developmental neurotoxicity. Environ. Res. 107, 45–52. https://doi.org/10.1016/j. envres.2007.07.006.

Chong, J., Liu, P., Zhou, G., Xia, J., 2020. Using MicrobiomeAnalyst for comprehensive statistical, functional, and meta-analysis of microbiome data. Nat. Protoc. 15, 799–821. https://doi.org/10.1038/s41596-019-0264-1.

Collado, M.C., Rautava, S., Isolauri, E., Salminen, S., 2015. Gut microbiota: A source of novel tools to reduce the risk of human disease. Pediatr. Res. 77, 182–188. https:// doi.org/10.1038/pr.2014.173.

D'Amato, A., Di Cesare Mannelli, L., Lucarini, E., Man, A.L., Le Gall, G., Branca, J.J.V., Ghelardini, C., Amedei, A., Bertelli, E., Regoli, M., Vauzour, D., Nicoletti, C., 2020. Faecal microbiota transplant from aged donor mice affects spatial learning and memory via modulating hippocampal synaptic plasticity- And neurotransmission-related proteins in young recipients. Microbiome 8. https://doi.org/10.1186/ s40168-020-00914-w.

Dobranowski, P.A., Tang, C., Sauvé, J.P., Menzies, S.C., Sly, L.M., 2019. Compositional changes to the ileal microbiome precede the onset of spontaneous ileitis in SHIP deficient mice. Gut Microbes 10, 578–598. https://doi.org/10.1080/ 19490976.2018.1560767.

Ezeji, J.C., Sarikonda, D.K., Hopperton, A., Erkkila, H.L., Cohen, D.E., Martinez, S.P., Cominelli, F., Kuwahara, T., Dichosa, A.E.K., Good, C.E., Veloo, A., Rodriguez-Palacios, A., 2021. Parabacteroides distasonis: intriguing aerotolerant gut anaerobe with emerging antimicrobial resistance and pathogenic and probiotic roles in human health. Gut Microbes 13. https://doi.org/10.1080/19490976.2021.1922241.

Fekadu, S., Alemayehu, E., Dewil, R., Van der Bruggen, B., 2019. Pharmaceuticals in freshwater aquatic environments: A comparison of the African and European challenge. Sci. Total Environ. 654, 324–337. https://doi.org/10.1016/j. scitotenv.2018.11.072.

Flora, S.J.S., Behari, J.R., Ashquin, M., Tandon, S.K., 1982. Time-dependent protective effect of selenium against cadmium-induced nephrotoxicity and hepatotoxicity. Chem. Biol. Interact. 42, 345–351. https://doi.org/10.1016/0009-2797(82)90078-3.

García-Barrera, T., Rodríguez-Moro, G., Callejón-Leblic, B., Arias-Borrego, A., Gómez-Ariza, J.L., 2018. Mass spectrometry based analytical approaches and pitfalls for toxicometabolomics of arsenic in mammals: A tutorial review. Anal. Chim. Acta 1000, 41–66. https://doi.org/10.1016/j.aca.2017.10.019.

García-Barrera, T., Gómez-Ariza, J.L., González-Fernández, M., Moreno, F., García-Sevillano, M.A., Gómez-Jacinto, V., 2012. Biological responses related to agonistic, antagonistic and synergistic interactions of chemical species. Anal. Bioanal. Chem. 403, 2237–2253. https://doi.org/10.1007/s00216-012-5776-2.

García-Sevillano, M.A., García-Barrera, T., Gómez-Ariza, J.L., 2014b. Application of metallomic and metabolomic approaches in exposure experiments on laboratory mice for environmental metal toxicity assessment. Metallomics 6, 237–248. https:// doi.org/10.1039/c3mt00302g.

García-Sevillano, M.A., García-Barrera, T., Gómez-Ariza, J.L., 2014c. Simultaneous speciation of selenoproteins and selenometabolites in plasma and serum by dual size exclusion-affinity chromatography with online isotope dilution inductively coupled plasma mass spectrometry. Anal. Bioanal. Chem. 406, 2719–2725. https://doi.org/ 10.1007/s00216-014-7629-7.

García-Sevillano, M.A., García-Barrera, T., Navarro, F., Gómez-Ariza, J.L., 2013. Analysis of the biological response of mouse liver (Mus musculus) exposed to As$_2$O$_3$ based on integrated -omics approaches. Metallomics 5, 1644–1655. https://doi.org/10.1039/c3mt00186e.

García-Sevillano, M.A., Contreras-Acuña, M., García-Barrera, T., Navarro, F., Gómez-Ariza, J.L., 2014a. Metabolomic study in plasma, liver and kidney of mice exposed to inorganic arsenic based on mass spectrometry. Anal. Bioanal. Chem. 406, 1455–1469. https://doi.org/10.1007/s00216-013-7564-z.

García-Sevillano, M.A., Rodríguez-Moro, G., García-Barrera, T., Navarro, F., Gómez-Ariza, J.L., 2015. Biological interactions between mercury and selenium in distribution and detoxification processes in mice under controlled exposure. Effects on selenoprotein. Chem. Biol. Interact. 229, 82–90. https://doi.org/10.1016/J. CBI.2015.02.001.

George, C.M., Gamble, M., Slavkovich, V., Levy, D., Ahmed, A., Ahsan, H., Graziano, J., 2013. A cross-sectional study of the impact of blood selenium on blood and urinary

arsenic concentrations in Bangladesh. Environ. Heal. A Glob. Access Sci. Source 12. https://doi.org/10.1186/1476-069X-12-52.

González-Gaya, B., García-Bueno, N., Buelow, E., Marin, A., Rico, A., 2022. Effects of aquaculture waste feeds and antibiotics on marine benthic ecosystems in the Mediterranean Sea. Sci. Total Environ. 806 https://doi.org/10.1016/j.scitotenv.2021.151190.

Hadley Wickham, Elegant Graphics for Data Analysis, in: Ggplot2, 1st ed., Springer, New York, NY, HoustonU.S.A., 2009: pp. VIII, 213. doi:https://doi.org/10.1007/978-0-387–98141-3.

Hayakawa, T., Kobayashi, Y., Cui, X., Hirano, S., 2005. A new metabolic pathway of arsenite: Arsenic-glutathione complexes are substrates for human arsenic methyltransferase Cyt19. Arch. Toxicol. 79, 183–191. https://doi.org/10.1007/s00204-004-0620-x.

Hu, Z.P., Browne, E.R., Liu, T., Angel, T.E., Ho, P.C., Chan, E.C.Y., 2012. Metabonomic profiling of TASTPM transgenic Alzheimer's disease mouse model. J. Proteome Res. 11, 5903–5913. https://doi.org/10.1021/pr300666p.

Huygens, J., Rasschaert, G., Heyndrickx, M., Dewulf, J., Van Coillie, E., Quataert, P., Daeseleire, E., Becue, I., 2022. Impact of fertilization with pig or calf slurry on antibiotic residues and resistance genes in the soil. Sci. Total Environ. 822 https://doi.org/10.1016/j.scitotenv.2022.153518.

J.-K.H.Menq-Rong Wu, Te-Sen Chou, Ching-Ying Huang, A potential probiotic-Lachnospiraceae NK4A136 group: Evidence from the restoration of the dietary pattern from a high-fat diet, Angew. Chemie Int. Ed. 6(11), 951–952, 2021: 2013–2015. https://doi.org/10.21203/rs.3.rs-48913/v1.

John Quensen, Make ggplot Versions of Vegan's Ordiplots, 2020. ⟨http://github.com/jfq3/ggordiplots⟩.

Kashida, Y., Takahashi, A., Moto, M., Okamura, M., Muguruma, M., Jin, M., Arai, K., Mitsumori, K., 2006. Gene expression analysis in mice liver on hepatocarcinogenesis by flumequine. Arch. Toxicol. 80, 533–539. https://doi.org/10.1007/s00204-006-0065-5.

Kaur, H., Bose, C., Mande, S.S., 2019. Tryptophan Metabolism by Gut Microbiome and Gut-Brain-Axis: An in silico Analysis. Front. Neurosci. 13 https://doi.org/10.3389/fnins.2019.01365.

Kolachi, N.F., Kazi, T.G., Wadhwa, S.K., Afridi, H.I., Baig, J.A., Khan, S., Shah, F., 2011. Evaluation of selenium in biological sample of arsenic exposed female skin lesions and skin cancer patients with related to non-exposed skin cancer patients. Sci. Total Environ. 409, 3092–3097. https://doi.org/10.1016/j.scitotenv.2011.05.008.

López-Pacheco, I.Y., Silva-Núñez, A., Salinas-Salazar, C., Arévalo-Gallegos, A., Lizarazo-Holguin, L.A., Barceló, D., Iqbal, H.M.N., Parra-Saldívar, R., 2019. Anthropogenic contaminants of high concern: Existence in water resources and their adverse effects. Sci. Total Environ. 690, 1068–1088. https://doi.org/10.1016/j.scitotenv.2019.07.052.

McMurdie, P.J., Holmes, S., 2013. Phyloseq: an R package for reproducible interactive analysis and graphics of microbiome census data. PLoS One 8. https://doi.org/10.1371/journal.pone.0061217.

Messaoudi, I., El Heni, J., Hammouda, F., Saïd, K., Kerkeni, A., 2009. Protective effects of selenium, zinc, or their combination on cadmium-induced oxidative stress in rat kidney. Biol. Trace Elem. Res. 130, 152–161. https://doi.org/10.1007/s12011-009-8324-y.

Milošević, M.D., Paunović, M.G., Matić, M.M., Ognjanović, B.I., Saičić, Z.S., 2017. The ameliorating effects of selenium and vitamin C against fenitrothion-induced blood toxicity in Wistar rats. Environ. Toxicol. Pharmacol. 56, 204–209. https://doi.org/10.1016/j.etap.2017.09.016.

Mostert, V., 2000. Selenoprotein P: Properties, functions, and regulation. Arch. Biochem. Biophys. 376, 433–438. https://doi.org/10.1006/abbi.2000.1735.

Mukherjee, A., Sharma, A., Talukder, G., 1988. Effect of selenium on cadmium-induced chromosomal aberrations in bone marrow cells of mice. Toxicol. Lett. 41, 23–29. https://doi.org/10.1016/0378-4274(88)90004-5.

Nguyen, M.H., Pham, T.D., Nguyen, T.L., Vu, H.A., Ta, T.T., Tu, M.B., Nguyen, T.H.Y., Chu, D.B., 2018. Speciation analysis of arsenic compounds by HPLC-ICP-MS: application for human serum and urine. J. Anal. Methods Chem. 2018 https://doi.org/10.1155/2018/9462019.

Nguyen, T.D., Prykhodko, O., Fåk Hållenius, F., Nyman, M., 2019. Monovalerin and trivalerin increase brain acetic acid, decrease liver succinic acid, and alter gut microbiota in rats fed high-fat diets. Eur. J. Nutr. 58, 1545–1560. https://doi.org/10.1007/s00394-018-1688-z.

Nordberg, G.F., Jin, T., Hong, F., Zhang, A., Buchet, J.P., Bernard, A., 2005. Biomarkers of cadmium and arsenic interactions. Toxicol. Appl. Pharmacol. 206, 191–197. https://doi.org/10.1016/J.TAAP.2004.11.028.

Owumi, S.E., Aliyu-Banjo, N.O., Odunola, O.A., 2020. Selenium attenuates diclofenac-induced testicular and epididymal toxicity in rats. Andrologia 52. https://doi.org/10.1111/and.13669.

Park, K., Mozaffarian, D., 2010. Omega-3 fatty acids, mercury, and selenium in fish and the risk of cardiovascular diseases. Curr. Atheroscler. Rep. 12, 414–422. https://doi.org/10.1007/s11883-010-0138-z.

Pepper, M.P., Vatamaniuk, M.Z., Yan, X., Roneker, C.A., Lei, X.G., 2011. Impacts of dietary Selenium deficiency on metabolic phenotypes of diet-restricted GPX1-overexpressing mice. Antioxid. Redox Signal 14, 383–390. https://doi.org/10.1089/ars.2010.3295.

R. Core Team, R: A language and environment for statistical computing. R Foundation for Statistical Computing, Vienna, Austria, 2020. http://www.r-project.org/index.html.

R.K. Jari Oksanen, F.Guillaume Blanchet, Michael Friendly, R.B.O.Pierre Legendre, Dan McGlinn, Peter R. Minchin, E.S. Gavin L. Simpson, Peter Solymos, M. Henry H. Stevens, H. Wagner, Package 'vegan'.Community Ecology Package, 2020.

Ramírez-Acosta, S., Selma-Royo, M., Collado, M.C., Navarro-Roldán, F., Abril, N., García-Barrera, T., 2022. Selenium supplementation influences mice testicular selenoproteins driven by gut microbiota. Sci. Rep. 12 https://doi.org/10.1038/s41598-022-08121-3.

Rasheed, H., Kay, P., Slack, R., Gong, Y.Y., 2019. Assessment of arsenic species in human hair, toenail and urine and their association with water and staple food. J. Expo. Sci. Environ. Epidemiol. 29, 624–632. https://doi.org/10.1038/s41370-018-0056-7.

Rayman, M.P., 2012. Selenium and human health. Lancet 379, 1256–1268. https://doi.org/10.1016/S0140-6736(11)61452-9.

Reichl, F.-X., Szinicz, L., Kreppel, H., Forth, W., 1988. Effect of arsenic on carbohydrate metabolism after single or repeated injection in guinea pigs. Arch. Toxicol. 62, 473–475. https://doi.org/10.1007/BF00288353.

Reichl, F.-X., Szinicz, L., Kreppel, H., Forth, W., 1989. Effects on mitochondrial metabolism in livers of guinea pigs after a single or repeated injection of As₂O₃. Arch. Toxicol. 63, 419–422. https://doi.org/10.1007/BF00303134.

Reid, G., 1999. The scientific basis for probiotic strains of Lactobacillus. Appl. Environ. Microbiol. 65, 3763–3766. https://doi.org/10.1128/aem.65.9.3763-3766.1999.

Rodríguez-González, P., Marchante-Gayón, J.M., García Alonso, J.I., Sanz-Medel, A., 2005. Isotope dilution analysis for elemental speciation: A tutorial review. Spectrochim. Acta - Part B . Spectrosc. 60, 151–207. https://doi.org/10.1016/j.sab.2005.01.005.

Rodríguez-Moro, G., Abril, N., Jara-Biedma, R., Ramírez-Acosta, S., Gómez-Ariza, J.L., García-Barrera, T., 2019. Metabolic Impairments Caused by a "chemical Cocktail" of DDE and Selenium in Mice Using Direct Infusion Triple Quadrupole Time-of-Flight and Gas Chromatography-Mass Spectrometry. Chem. Res. Toxicol. 32, 1940–1954. https://doi.org/10.1021/acs.chemrestox.9b00102.

Rodríguez-Moro, G., Roldán, F.N., Baya-Arenas, R., Arias-Borrego, A., Callejón-Leblic, B., Gómez-Ariza, J.L., García-Barrera, T., 2020. Metabolic impairments, metal traffic, and dyshomeostasis caused by the antagonistic interaction of cadmium and selenium using organic and inorganic mass spectrometry. Environ. Sci. Pollut. Res. 27, 1762–1775. https://doi.org/10.1007/s11356-019-06573-1.

S.S. Leo Lahti, microbiome R package, 2017. ⟨http://microbiome.github.io⟩.

Saito, Y., 2021. Selenium Transport Mechanism via Selenoprotein P—Its Physiological Role and Related Diseases. Front. Nutr. 8, 1–7. https://doi.org/10.3389/fnut.2021.685517.

Sanz-Medel, A., 2016. "Heteroatom-tagged" quantification of proteins via ICP-MS. Anal. Bioanal. Chem. 408, 5393–5395. https://doi.org/10.1007/s00216-016-9687-5.

Suzuki, Y., Hashiura, Y., Sakai, T., Yamamoto, T., Matsukawa, T., Shinohara, A., Furuta, N., 2013. Selenium metabolism and excretion in mice after injection of 82Se-enriched selenomethionine. Metallomics 5, 445–452. https://doi.org/10.1039/c3mt20267d.

Szinicz, L., Forth, W., 1988. Effect of As₂O₃ on gluconeogenesis. Arch. Toxicol. 61, 444–449. https://doi.org/10.1007/BF00293690.

Thorsten Pohlert, P.M.C.M.Rplus: Calculate Pairwise Multiple Comparisons of Mean Rank Sums Extended. R package, 2021. ⟨https://cran.r-project.org/package=PMCMRplus⟩.

Tian, T., Xu, B., Qin, Y., Fan, L., Chen, J., Zheng, P., Gong, X., Wang, H., Bai, M., Pu, J., Lu, J., Zhou, W., Zhao, L., Yang, D., Xie, P., 2019a. Clostridium butyricum miyairi 588 has preventive effects on chronic social defeat stress-induced depressive-like behaviour and modulates microglial activation in mice. Biochem. Biophys. Res. Commun. 516, 430–436. https://doi.org/10.1016/J.BBRC.2019.06.053.

Tian, X., Yu, Z., Feng, P., Ye, Z., Li, R., Liu, J., Hu, J., Kakade, A., Liu, P., Li, X., 2019b. Lactobacillus plantarum TW1-1 alleviates diethylhexylphthalate-induced testicular damage in mice by modulating gut microbiota and decreasing inflammation. Front. Cell. Infect. Microbiol. 9 https://doi.org/10.3389/fcimb.2019.00221.

Torres-Sánchez, L., López-Carrillo, L., Rosado, J.L., Rodriguez, V.M., Vera-Aguilar, E., Kordas, K., García-Vargas, G.G., Cebrian, M.E., 2016. Sex differences in the reduction of arsenic methylation capacity as a function of urinary total and inorganic arsenic in Mexican children. Environ. Res. 151, 38–43. https://doi.org/10.1016/J.ENVRES.2016.07.020.

Trombini, C., Kazakova, J., Montilla-López, A., Fernández-Cisnal, R., Hampel, M., Fernández-Torres, R., Bello-López, M.Á., Abril, N., Blasco, J., 2021. Assessment of pharmaceutical mixture (ibuprofen, ciprofloxacin and flumequine) effects to the crayfish Procambarus clarkii: A multilevel analysis (biochemical, transcriptional and proteomic approaches). Environ. Res. 200 https://doi.org/10.1016/j.envres.2021.111396.

Vahter, M., 1999. Methylation of inorganic arsenic in different mammalian species and population groups. Sci. Prog. 82 (Pt 1), 69–88. https://doi.org/10.1177/003685049908200104.

Van Genderen, E., Adams, W., Dwyer, R., Garman, E., Gorsuch, J., 2015. Modeling and interpreting biological effects of mixtures in the environment: Introduction to the metal mixture modeling evaluation project. Environ. Toxicol. Chem. 34, 721–725. https://doi.org/10.1002/etc.2750.

Villaseñor, A., Garcia-Perez, I., Garcia, A., Posma, J.M., Fernández-López, M., Nicholas, A.J., Modi, N., Holmes, E., Barbas, C., 2014. Breast milk metabolome characterization in a single-phase extraction, multiplatform analytical approach. Anal. Chem. 86, 8245–8252. https://doi.org/10.1021/ac501853d.

Xu, F., Cheng, Y., Ruan, G., Fan, L., Tian, Y., Xiao, Z., Chen, D., Wei, Y., 2021. New pathway ameliorating ulcerative colitis: focus on Roseburia intestinalis and the gut–brain axis. Ther. Adv. Gastroenterol. 14 https://doi.org/10.1177/17562848211004469.

Xu, Y., Li, H., Chen, W., Yao, X., Xing, Y., Wang, X., Zhong, J., Meng, G., 2013. Mycoplasma hyorhinis activates the NLRP3 inflammasome and promotes migration and invasion of gastric chancer cells. PLoS One 8. https://doi.org/10.1371/journal.pone.0077955.

Yáñez, L., Carrizales, L., Zanatta, M.T., de Jesús Mejía, J., Batres, L., Díaz-Barriga, F., 1991. Arsenic-cadmium interaction in rats: toxic effects in the heart and tissue metal shifts. Toxicology 67, 227–234. https://doi.org/10.1016/0300-483X(91)90145-Q.

Yang, C., Chalasani, G., Ng, Y.-H., Robbins, P.D., 2012. Exosomes released from mycoplasma infected tumor cells activate inhibitory B cells. PLoS One 7. https://doi.org/10.1371/journal.pone.0036138.

Yim, Y.-J., Seo, J., Kang, S.-I., Ahn, J.-H., Hur, H.-G., 2008. Reductive dechlorination of methoxychlor and DDT by human intestinal bacterium Eubacterium limosum under anaerobic conditions. Arch. Environ. Contam. Toxicol. 54, 406–411. https://doi.org/10.1007/s00244-007-9044-y.

Zarrinpar, A., Chaix, A., Xu, Z.Z., Chang, M.W., Marotz, C.A., Saghatelian, A., Knight, R., Panda, S., 2018. Antibiotic-induced microbiome depletion alters metabolic homeostasis by affecting gut signaling and colonic metabolism. Nat. Commun. 9 https://doi.org/10.1038/s41467-018-05336-9.

Zhai, Q., Cen, S., Li, P., Tian, F., Zhao, J., Zhang, H., Chen, W., 2018. Effects of Dietary Selenium Supplementation on Intestinal Barrier and Immune Responses Associated with Its Modulation of Gut Microbiota. Environ. Sci. Technol. Lett. 5, 724–730. https://doi.org/10.1021/acs.estlett.8b00563.

Zhai, Q., Li, T., Yu, L., Xiao, Y., Feng, S., Wu, J., Zhao, J., Zhang, H., Chen, W., 2017. Effects of subchronic oral toxic metal exposure on the intestinal microbiota of mice. Sci. Bull. 62, 831–840. https://doi.org/10.1016/j.scib.2017.01.031.